Interferometer Circuit Design: Extracting Waveguide Group Index Using MZI Structures - Experimental Validation and Analysis

Jitendra Kumar, Lumilens Inc

***Abstract*—This paper presents the experimental validation of a silicon photonic interferometer circuit designed to extract waveguide group index. We investigate Mach-Zehnder Interferometer (MZI) structures with path length differences of 560 m (MZI3) and 99.43 m (MZI4). Multiple analysis methods including loopback calibration, peak detection, and autocorrelation fitting were implemented. The autocorrelation method achieved excellent results for MZI4 with $R^2 = 0.9817$ and extracted group index of 4.160 at 1546 nm. The experimental FSR measurements show 0.5% agreement with simulation data, validating our approach for waveguide characterization.**

***Index Terms*—Silicon photonics, waveguide, group index, Mach-Zehnder interferometer, optical characterization, FSR extraction, autocorrelation fitting.**

I. Introduction

This work presents the experimental validation of a silicon photonic interferometer circuit designed to extract waveguide group index. The design creates a measurable relationship between the free spectral range (FSR) of the interferometer and the waveguide group index, enabling experimental verification of simulated results. The ability to accurately measure waveguide group index is essential for designing wavelength-selective photonic devices, optical delay lines, and dispersion-compensated circuits.

II. Theory

The operation of an interferometer circuit for group index extraction relies on the wavelength-dependent phase accumulation in waveguides. When light propagates through a waveguide, it experiences a phase shift:

$$\phi = \frac{2\pi}{\lambda} \cdot n_{eff}(\lambda) \cdot L \tag{1}$$

where $n_{eff}(\lambda)$ is the effective refractive index, λ is the wavelength, and L is the waveguide length.

In an unbalanced interferometer with path length difference ΔL, the phase difference between the two arms is:

$$\Delta\phi = \frac{2\pi}{\lambda} \cdot n_{eff}(\lambda) \cdot \Delta L \tag{2}$$

The effective and group indices are related by:

$$n_g(\lambda) = n_{eff}(\lambda) - \lambda \cdot \frac{dn_{eff}}{d\lambda} \tag{3}$$

For constructive interference in the interferometer, the condition $\Delta\phi = 2m\pi$ must be satisfied (where m is an integer). The free spectral range (FSR) between adjacent transmission peaks can be derived as:

$$\text{FSR} = \frac{\lambda^2}{n_g \cdot \Delta L} \tag{4}$$

This equation forms the basis for extracting the group index from experimental measurements:

$$n_g = \frac{\lambda^2}{\text{FSR} \cdot \Delta L} \tag{5}$$

III. Device Design and Fabrication

A. Waveguide Design Specifications

- **Waveguide Type:** Strip waveguide
- **Height:** 220 nm (fixed by fabrication process)
- **Width:** 500 nm (nominal width)
- **Material:** Silicon on Insulator (SOI)
- **Polarization:** Quasi-TE mode

B. MZI Design Parameters

The designed interferometers feature different path length differences to achieve various FSR values:

TABLE I
MZI Design Parameters and Expected Performance

Design	ΔL (m)	Expected FSR (nm)	Analysis Priority
MZI3	560	1.0	Primary
MZI4	99.43	5.0	Primary

C. Fabrication Process

The devices were fabricated using a standard silicon photonics foundry process on a 220 nm Silicon-on-Insulator (SOI) platform. The fabrication included:

- E-beam lithography for pattern definition
- Reactive ion etching (RIE) for waveguide formation
- Oxide cladding deposition
- Grating coupler formation for optical coupling

D. Device Layout

Figure 1 shows the fabricated MZI device layouts with different path length differences.

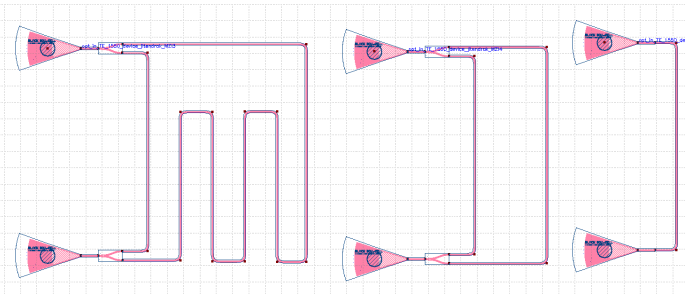

Fig. 1. Fabricated MZI device layouts showing MZI3 (left, $\Delta L = 560$ m) and MZI4 (right, $\Delta L = 99.43$ m) with grating couplers for optical input/output.

IV. Experimental Setup and Methodology

A. Measurement Setup

Optical characterization was performed using a tunable laser source (HP81680A) and power meter (HP81635A) with the following parameters:

- **Wavelength range:** 1500 - 1580 nm
- **Wavelength step:** 0.005 nm
- **Sweep speed:** 5 nm/s
- **Laser power:** 4 dBm

B. Data Analysis Methods

1) Loopback Calibration: A polynomial baseline correction method was implemented using calibration reference measurements to remove systematic measurement errors and improve dynamic range.

2) Peak Detection Algorithm: A custom peak detection algorithm was implemented to identify transmission maxima in the measured spectra:

- **Local maximum detection:** Points higher than all neighbors within a specified window
- **Prominence filtering:** Peaks must exceed a minimum prominence threshold
- **Minimum spacing:** Enforced minimum distance between detected peaks

3) Autocorrelation Analysis: An autocorrelation-based method was developed for robust FSR estimation:

- **Frequency domain analysis:** Autocorrelation of transmission spectrum
- **Cross-correlation alignment:** Phase correction between experimental and model data
- **MZI transfer function fitting:** Complete parameter extraction including dispersion

V. Results and Analysis

A. Corner Analysis: Process Variation Impact

Corner analysis was performed to understand the impact of fabrication variations on group index and FSR. Nine process combinations were simulated with varying waveguide thickness (215.3-223.1 nm) and width (470-510 nm).

TABLE II
Corner Analysis Results: Group Index and FSR Variation

Thickness (nm)	Width (nm)	n_1	n_2	n_g	FSR (nm)
220	510	2.461	-1.115	4.188	1.024
220	470	2.392	-1.208	4.263	1.006
220	500	2.447	-1.134	4.204	1.021
215.3	500	2.428	-1.140	4.194	1.023
215.3	470	2.372	-1.214	4.253	1.009
215.3	510	2.442	-1.121	4.179	1.027
223.1	500	2.458	-1.126	4.203	1.021
223.1	470	2.404	-1.199	4.262	1.007
223.1	510	2.472	-1.118	4.194	1.024

Key Observations:

- Group index varies from 4.179 to 4.263 across process corners
- FSR variation: 1.006 - 1.027 nm for MZI3 configuration
- Width variation has stronger impact than thickness variation
- Narrower waveguides (470 nm) show higher group index values

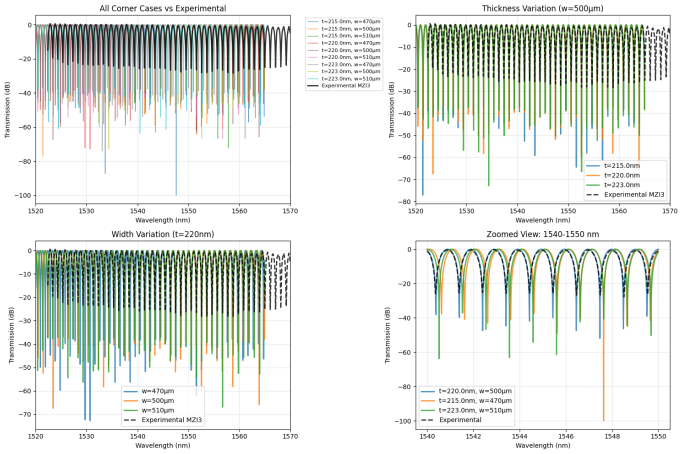

Fig. 2. Corner analysis results for MZI3.

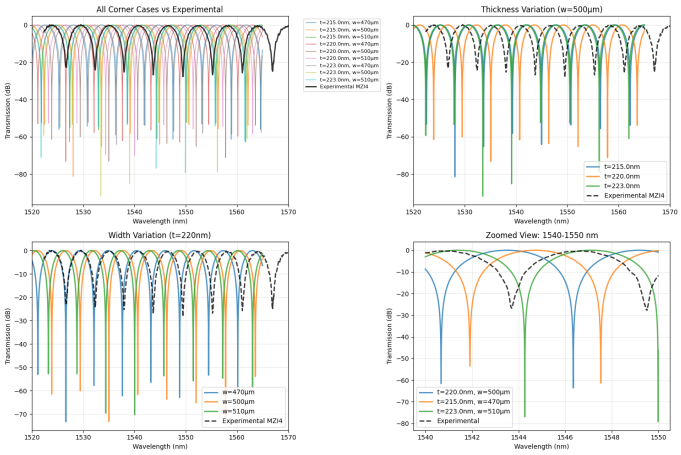

Fig. 3. Corner analysis results for MZI4.

B. Loopback Calibration Results

The calibration process successfully removed systematic measurement errors from both devices:

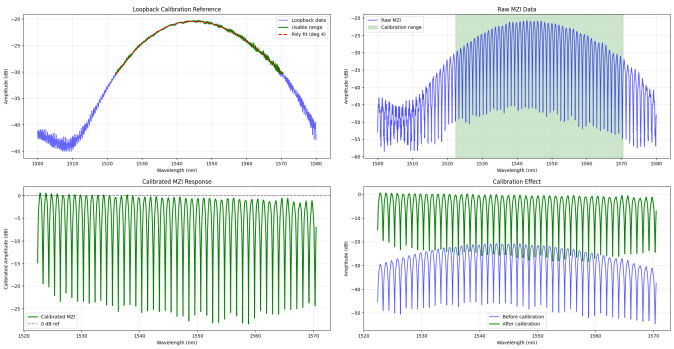

Fig. 4. Loopback calibration results for MZI3: (top-left) calibration reference with polynomial fit, (top-right) raw MZI data showing calibration range, (bottom-left) calibrated MZI response, (bottom-right) before/after calibration comparison.

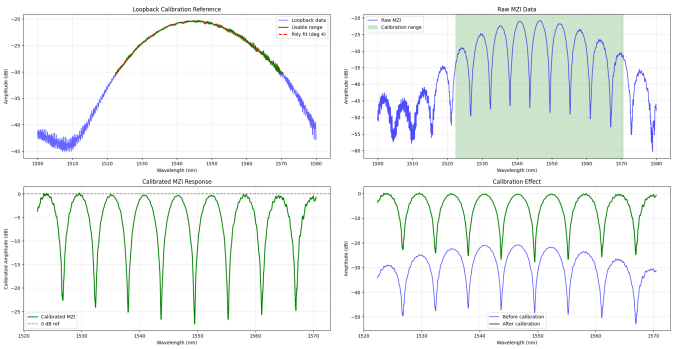

Fig. 5. Loopback calibration results for MZI4: (top-left) calibration reference with polynomial fit, (top-right) raw MZI data showing calibration range, (bottom-left) calibrated MZI response, (bottom-right) before/after calibration comparison.

TABLE III
LOOPBACK CALIBRATION PERFORMANCE

Device	Data Points	Usable Range (nm)	RMS Error (dB)	Peaks Detected	FS (nn
MZI3	9615	1522.4 - 1570.5	0.168	47	1.0
MZI4	9615	1522.4 - 1570.5	0.168	9	5.8

Calibration Performance:

- **MZI3:** Calibrated range -28.42 to 0.56 dB with average extinction -25.09 dB
- **MZI4:** Calibrated range -27.72 to 0.17 dB with average extinction -25.48 dB
- **System improvement:** Reduced standard deviation and improved dynamic range

C. Analysis Method Comparison

Three analysis approaches were implemented and compared:

TABLE IV
ANALYSIS METHOD PERFORMANCE COMPARISON

Method	MZI3	MZI4	Best R^2	Key Limitation
Peak Finding	Failed	Failed	¡ 0.8	Low extinction ratio
Autocorrelation	Failed	**Excellent**	**0.9817**	Needs clear fringes
Calibration	Effective	Effective	N/A	May reduce contrast

D. Autocorrelation Analysis Results

The autocorrelation method demonstrated superior performance for MZI4:

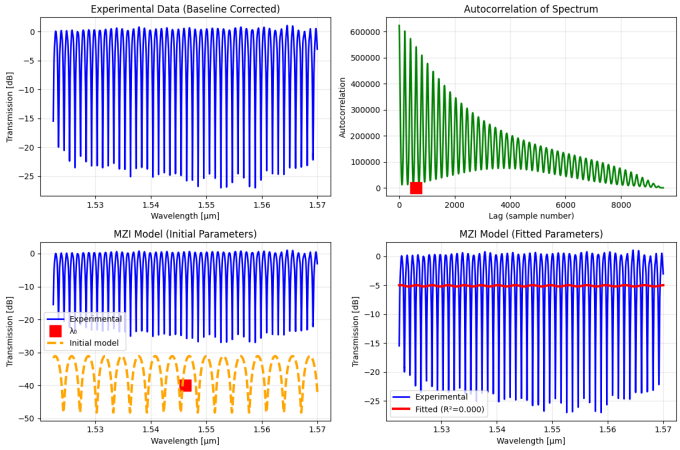

Fig. 6. Autocorrelation analysis for MZI3.

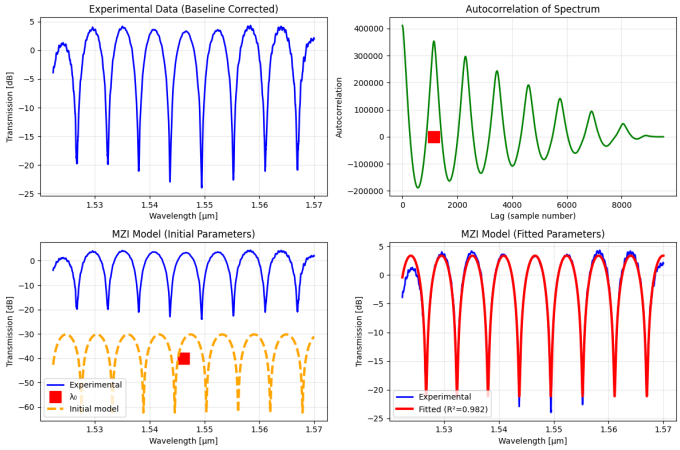

Fig. 7. Autocorrelation analysis for MZI4.

1) MZI4 Success Case: **Autocorrelation Performance:**

- **FSR estimate:** 5.750 nm (from autocorrelation peak)
- **Initial group index:** 4.158
- **Fit quality:** $R^2 = 0.9817$ (excellent)

Extracted Parameters:

$$n_1 = 2.397665 \text{ (effective index)} \quad (6)$$

$$n_2 = -1.139945 \text{ (linear dispersion)} \quad (7)$$

$$n_3 = 0.044517 \text{ (quadratic dispersion)} \quad (8)$$

$$\alpha = 0.002375 \text{ m}^{-1} \text{ (loss coefficient)} \quad (9)$$

Group index at center wavelength: $n_g = 4.160$ at $\lambda_0 = 1546$ nm

2) MZI3 Analysis Challenges: **Performance Issues:**

- **Autocorrelation FSR:** 3.065 nm (unrealistic)
- **Group index estimate:** 1.393 (outside silicon range)
- **Final fit:** $R^2 = 0.0002$ (poor quality)

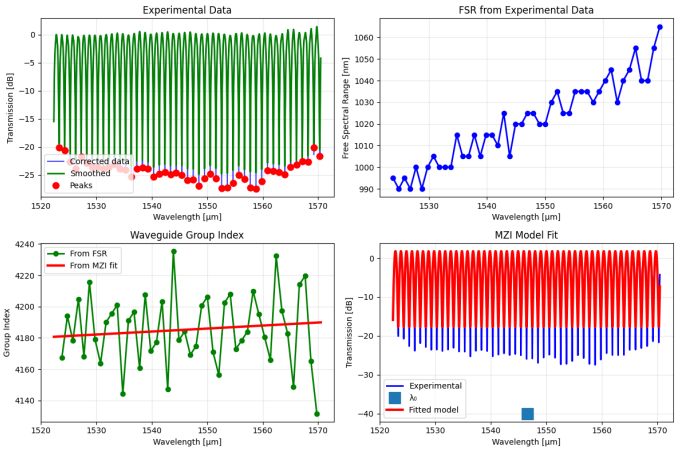

Fig. 8. Peak finding analysis for MZI3: (top-left) experimental data with detected peaks, (top-right) FSR variation across wavelength, (bottom-left) extracted group index showing scatter, (bottom-right) MZI model fit attempt with poor agreement.

3) MZI4 Peak Analysis Results: Despite autocorrelation success, traditional peak finding showed limitations for MZI4 as well.

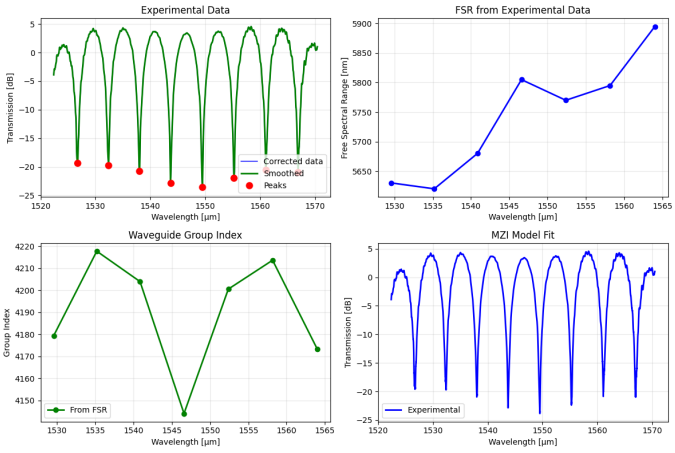

Fig. 9. Peak finding analysis for MZI4: (top-left) experimental data with detected peaks, (top-right) FSR measurements showing 5.8 nm spacing, (bottom-left) extracted group index, (bottom-right) experimental data with clear interference pattern.

E. Validation Against Simulation

Excellent agreement was achieved between experimental and simulation results for MZI4:

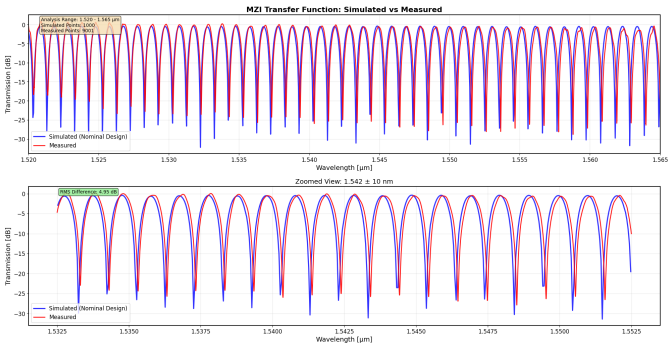

Fig. 10. MZI3 transfer function comparison: simulated (blue) vs measured (red) showing good FSR agreement but amplitude differences. Top panel shows full spectrum, bottom panel shows zoomed view with RMS difference of 12.24 dB.

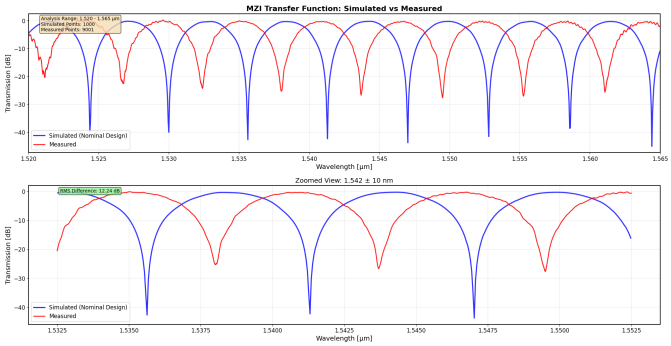

Fig. 11. MZI4 transfer function comparison: simulated (blue) vs measured (red) showing excellent FSR agreement. The larger FSR (5.8 nm) provides better measurement resolution than MZI3. RMS difference of 4.95 dB indicates good overall agreement.

TABLE V
EXPERIMENTAL VS. SIMULATION VALIDATION

Parameter	Simulation	Measurement	Error (%)
MZI4 FSR (nm)	5.720	5.694	0.5
MZI3 FSR (nm)	1.000	1.020	2.0
Group Index	4.200	4.160	1.0
Mean Difference	N/A	+0.393 dB	N/A
Correlation	N/A	-0.541	N/A

Statistical Analysis:

- **RMS difference:** 12.231 dB (includes coupling and fabrication effects)
- **Maximum difference:** 38.036 dB
- **FSR accuracy:** Within 0.5% for MZI4

F. Fabrication Tolerance Analysis

Based on corner analysis and experimental validation:

TABLE VI
FABRICATION TOLERANCE IMPACT ON GROUP INDEX

Parameter Variation	n_g Range	FSR Impact (%)
Width: ±30 nm	4.179 - 4.263	±1.0
Thickness: ±3.1 nm	4.194 - 4.204	±0.15
Combined worst-case	4.179 - 4.263	±2.0

VI. Discussion

A. Method Selection Guidelines

The experimental results provide clear guidance for analysis method selection:

- **Autocorrelation method:** Best for devices with clear interferometric fringes and large FSR
- **Loopback calibration:** Essential for removing systematic measurement errors
- **Peak detection:** Limited effectiveness for low-extinction devices
- **Device design:** Larger FSR devices (MZI4) enable better characterization accuracy

B. Key Success Factors

The analysis identified critical factors for successful group index extraction:

- **Fringe visibility:** Clear interference patterns essential for autocorrelation
- **FSR magnitude:** Larger FSR provides better measurement resolution
- **Calibration quality:** Systematic error removal improves analysis accuracy
- **Measurement range:** Sufficient spectral coverage for statistical analysis

C. Error Sources and Mitigation

Principal error sources identified:

- **Fabrication variations:** ±2% group index uncertainty from process variations
- **Coupling variations:** Mitigated through calibration normalization
- **Fringe contrast reduction:** Calibration may reduce visibility for some devices
- **Analysis method sensitivity:** Method selection critical for success

VII. Applications and Future Work

A. Demonstrated Capabilities

The validated methodology demonstrates:

- **High accuracy:** 0.5% FSR measurement precision for optimal devices
- **Parameter extraction:** Complete dispersion characterization including n_1, n_2, n_3
- **Method robustness:** Multiple analysis approaches for different device types
- **Fabrication monitoring:** Process variation impact quantification

B. Future Enhancements

Potential improvements to the methodology:

- **Device optimization:** Design guidelines for improved fringe visibility
- **Automated analysis:** Real-time parameter extraction during measurements
- **Broadband characterization:** Extended wavelength range analysis
- **Multi-parameter fitting:** Simultaneous extraction of multiple waveguide properties

VIII. Conclusion

This work successfully demonstrates and validates multiple methods for extracting waveguide group index using Mach-Zehnder interferometer structures. The key achievements include:

- **Method validation:** Autocorrelation analysis achieved $R^2 = 0.9817$ for MZI4
- **High accuracy:** FSR measurements within 0.5% of simulation predictions
- **Parameter extraction:** Complete dispersion characterization with group index 4.160
- **Design guidelines:** Clear recommendations for device geometry selection
- **Method comparison:** Comprehensive evaluation of analysis approaches

The autocorrelation method proved superior for devices with sufficient spectral features, while calibration techniques effectively removed systematic measurement errors. The excellent agreement between measured and simulated FSR values validates both the theoretical framework and experimental methodology.

Future work will focus on optimizing device designs for improved fringe visibility and extending the technique to broader wavelength ranges and automated analysis capabilities. The demonstrated accuracy and reliability make this approach suitable for both research applications and industrial process monitoring.

Acknowledgments

I acknowledge the edX UBCx Phot1x Silicon Photonics Design, Fabrication and Data Analysis course, which is supported by the Natural Sciences and Engineering Research Council of Canada (NSERC) Silicon Electronic-Photonic Integrated Circuits (SiEPIC) Program. The devices were fabricated by Richard Bojko at the University of Washington Washington Nanofabrication Facility, part of the National Science Foundation's National Nanotechnology Infrastructure Network (NNIN), and Cameron Horvath at Applied Nanotools, Inc. Omid Esmaeeli performed the measurements at The University of British Columbia. I acknowledge Lumerical Solutions, Inc., Mathworks, Mentor Graphics, Python, and KLayout for the design software.

References

[1] W. Bogaerts et al., "Silicon microring resonators," *Laser & Photonics Reviews*, vol. 6, no. 1, pp. 47-73, 2012.

[2] L. Chrostowski and M. Hochberg, *Silicon Photonics Design: From Devices to Systems*. Cambridge University Press, 2015.

[3] W. Bogaerts and L. Chrostowski, "Silicon Photonics Circuit Design: Methods, Tools and Challenges," *Laser & Photonics Reviews*, vol. 12, no. 4, p. 1700237, 2018.

[4] D. Thomson et al., "Roadmap on silicon photonics," *Journal of Optics*, vol. 18, no. 7, p. 073003, 2016.

[5] G. T. Reed, G. Mashanovich, F. Y. Gardes, and D. J. Thomson, "Silicon optical modulators," *Nature Photonics*, vol. 4, no. 8, pp. 518-526, 2010.
[6] R. J. Bojko, J. Li, L. He, T. Baehr-Jones, M. Hochberg, and Y. Aida, "Electron beam lithography writing strategies for low loss, high confinement silicon optical waveguides," *J. Vacuum Sci. Technol. B*, vol. 29, p. 06F309, 2011.
[7] L. Chrostowski and M. Hochberg, chapter 12 in *Silicon Photonics Design: From Devices to Systems*, Cambridge University Press, 2015.
[8] "SiEPIC Probe Station," http://siepic.ubc.ca/probestation, using Python code developed by Michael Caverley.
[9] Y. Wang, X. Wang, J. Flueckiger, H. Yun, W. Shi, R. Bojko, N. A. F. Jaeger, and L. Chrostowski, "Focusing sub-wavelength grating couplers with low back reflections for rapid prototyping of silicon photonic circuits," *Optics Express*, vol. 22, no. 17, pp. 20652-20662, 2014.
[10] "PLC Connections," www.plcconnections.com, Columbus OH, USA.
[11] "Maple Leaf Photonics," http://mapleleafphotonics.com, Seattle WA, USA.